Polymer Journal (2019) 51:365–370
https://doi.org/10.1038/s41428-018-0121-z

NOTE

Molecular dynamics study of the molecular mobilities and side-chain terminal affinities of 2-methoxyethyl acrylate and 2-hydroxyethyl methacrylate

Ryo Nagumo[1] · Atsushi Shimizu[1] · Shuichi Iwata[1] · Hideki Mori[1]

Received: 1 May 2018 / Revised: 8 August 2018 / Accepted: 9 August 2018 / Published online: 10 September 2018

Introduction

Nonfouling and biocompatible polymer surfaces and interfaces are essential for biomedical applications, marine coatings, and membrane separation processes for water treatment. Tanaka et al. reported that nonionic poly(2-methoxyethyl acrylate) (PMEA) and poly(2-hydroxyethyl methacrylate) (PHEMA) similarly inhibited protein adsorption, unlike poly(2-hydroxyethyl acrylate) (PHEA), but PMEA markedly suppressed platelet adhesion, unlike PHEMA [1]. To determine the reason for the superior blood compatibility of PMEA, Tanaka et al. focused on the interactions between water molecules and proteins using the "intermediate water" concept [2–5]. In these studies, intermediate water was hypothesized to prevent direct contact between proteins and/or platelets and the polymer surface. Seo et al. reported that molecular mobility was a significant factor that regulated the cellular response of polyrotaxane-based block copolymers [6]; consequently, molecular mobility is also likely to be a significant factor that determines the blood compatibilities of PMEA and PHEMA. Determining the reasons for the different blood compatibilities of PMEA and PHEMA will provide detailed insight into the antifouling/fouling mechanisms of nonionic polymer surfaces.

Molecular dynamics (MD) is a powerful approach that provides molecular-level information, including information regarding the microscopic behavior of water molecules on polymer surfaces [7]. Free-energy calculations were performed on PMEA and PHEMA to evaluate their protein resistance [8–10], which revealed that the affinities of the repeating units were significant factors that determined whether protein adsorption could be inhibited. As PMEA has been experimentally shown to be significantly more blood-biocompatible than PHEMA and PHEA [1], it is most likely that the affinities of the terminal methoxy groups in PMEA are inherently different from those of the terminal hydroxyl groups in PHEMA and PHEA. In this study, we evaluated the influence of the methoxy groups on the behavior of the foulant molecules by referring to our recent approach using zwitterionic moieties in which an organic solvent (*n*-hexane) was used as a simplified probe foulant [11]. In this work, 1-octanol, terminated by a polar hydroxyl group and a nonpolar methyl group, was adopted as the probe foulant. Thus, we were able to estimate the affinities of the terminal functional groups of 2-methoxyethyl acrylate (MEA) and 2-hydroxyethyl methacrylate (HEMA) using the polar groups of the probe foulants, as well as those with nonpolar groups. By comparing the structural and dynamic properties of the MEA/HEMA moieties in 1-octanol, in this study, we aimed to clarify the molecular mobilities of MEA/HEMA oligomers and the affinities of the side-chain terminal groups at the atomic level.

Materials and methods

The chemical structures of MEA and HEMA oligomers are shown in Fig. 1. Labels are assigned to the constituent atoms as follows: O_M and C_M denote oxygen and carbon atoms, respectively, in the terminal methoxy groups of the

Electronic supplementary material The online version of this article (https://doi.org/10.1038/s41428-018-0121-z) contains supplementary material, which is available to authorized users.

✉ Ryo Nagumo
nagumo@nitech.ac.jp

[1] Department of Life Science and Applied Chemistry, Nagoya Institute of Technology, Gokiso-cho, Showa-ku, Nagoya 466-8555, Japan

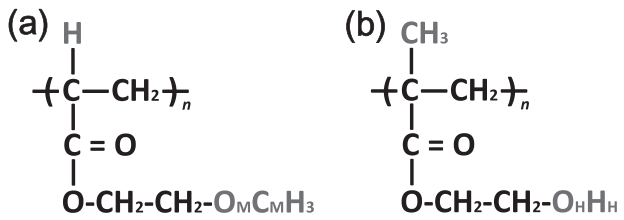

Fig. 1 Chemical structures of the **a** MEA and **b** HEMA moieties

MEA moieties; O_H and H_H denote oxygen and hydrogen atoms, respectively, in the terminal hydroxyl groups of HEMA moieties; O_O and H_O denote oxygen and hydrogen atoms, respectively, in the terminal hydroxyl groups of 1-octanol; and Co denotes the carbon atom in the terminal methyl group of 1-octanol. The molecular weights of the MEA and HEMA moieties are equal when they are polymerized to the same degree, n. In this work, moieties with polymerization of $n = 1$–5 were used in the MD simulations. The simulation system was a cubic box containing MEA or HEMA moieties with the same value of n and 1-octanol molecules; the solvent content was set to ~50 wt%. We aimed to evaluate the direct contact between the terminal groups of the MEA/HEMA side chains and the polar and nonpolar groups of the foulant molecules on the material–foulant interface by excluding the surrounding water molecules in the simulation cells.

Simulations of the oligomers ($n \geq 2$) were conducted using the AMBER 16 simulation package [12]: AMBER 12 was also used to simulate MEA/HEMA monomers as we previously reported [11]. Although different versions of the package were used, the results were not significantly influenced because identical simulation conditions were used, as described below. A generalized AMBER force field [13] was used to describe the bonding and nonbonding interactions between the MEA/HEMA moieties and 1-octanol, the atomic partial charges of which were assigned using the AM1-BCC method [14, 15]. After energy minimization, an equilibration MD simulation was performed with a 1-fs time step in the isobaric–isothermal (NPT) ensemble, which was terminated when the volume (density) of the simulation cell became almost constant. During the MD simulation in the NPT ensemble, the system was maintained at 300 K (1.0 ps time constant) and 1 bar (1.0 ps pressure relaxation time) using the Berendsen weak-coupling algorithm [16]. Following energy equilibration, another MD simulation was performed in the canonical ensemble with a 1-fs time step for data sampling, where the system was maintained at 300 K (1.0 ps time constant) using the Berendsen algorithm [16]. Van der Waals interactions were calculated with a cutoff distance of 10 Å, and long-range electrostatic interactions were calculated using the particle mesh Ewald method with periodic boundary conditions in three dimensions [17]. The default values in the AMBER package were used in the MD calculations for all other simulations. The numbers of MEA/HEMA moieties and solvent molecules in the simulation cubic cells, cell lengths, densities, and computational times for data sampling are given in Table S1. The densities (at room temperature) of 1-octanol, MEA monomer, and HEMA monomer were 0.8218 [18], 1.012 [19], and 1.073 g/cm^3 [20], and the cell densities of the systems listed in Table S1 were reasonable.

Following MD simulations of these systems, three properties were determined, namely, the molecular mobilities, solvation-density profiles, and binding strengths between the moieties and the solvent. The molecular mobilities of the MEA/HEMA moieties and the 1-octanol molecules were determined by calculating their self-diffusivities using the mean-square displacement (MSD) from Einstein's equation:

$$D = \frac{\left\langle |r(t) - r(t_0)|^2 \right\rangle}{6(t - t_0)} \tag{1}$$

where <…> denotes an ensemble average, $r(t)$ is the position of the molecule at time t, and t_0 is the initial data-sampling time. The MSD data from the final several nanoseconds of each MD run were used to calculate the diffusivities. The sampling times for the MSDs are also given in Table S1. Solvation-density profiles were calculated near the terminal groups of the MEA/HEMA moieties using radial distribution functions (RDFs). In this work, the RDFs were calculated for moieties with $n = 1$, 3, and 5. For the oligomers, we evaluated the RDFs near the terminal groups of the second repeat units (for trimers) and third repeat units (for pentamers).

To quantify the affinities between the functional groups of the solvates and those of the solvents, the binding strengths between the terminal groups of the MEA/HEMA moieties and those of the 1-octanol molecules were determined by calculating the "residence rate," which is defined by

$$C_r(t) = \frac{N(t)}{N(0)} \tag{2}$$

where $N(t)$ is the number of specific constituent atoms of 1-octanol molecules that remain in a sphere of radius r centered on a certain type of constituent atom of an MEA/HEMA moiety for time t without leaving the sphere. $N(t)$ was counted during 9.99 ps for all of the same type of atoms initially contained in that sphere. To ensure sufficient sampling, we determined $C_r(t)$ by calculating the average values of $N(t)/N(0)$ for numerous samples over 9.99 ps for multiple central atoms. The calculated $C_r(t)$ values were fitted by an exponential polynomial function to obtain the

residence time τ:

$$C_r(t) = c_1 \exp\left(-\frac{t}{\tau_1}\right) + c_2 \exp\left(-\frac{t}{\tau_2}\right) + c_3 \exp\left(-\frac{t}{\tau_3}\right) \quad (3)$$

$$\tau = c_1\tau_1 + c_2\tau_2 + c_3\tau_3 \quad (4)$$

where τ_k ($k = 1, 2, 3$) and c_k are the fitting parameters (the sum of $c_k = 1$) and τ represents the average time that the constituent atoms of the 1-octanol molecules remain in the immediate vicinity of the terminal groups of a moiety during the MD simulations. In other words, τ is a criterion of the binding strength between the MEA/HEMA moieties and the 1-octanol molecules at the atomic level, and τ is dependent on the set value of radius r.

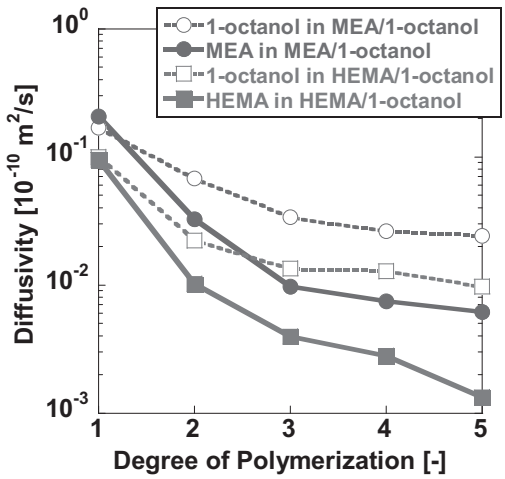

Fig. 2 Relationships between the degree of polymerization of MEA/HEMA moieties and the self- diffusivity of each component at 300 K in mixtures of MEA/HEMA moieties and 1-octanol molecules

Results

The self-diffusivity of each component was calculated to evaluate the molecular mobility of the MEA/HEMA moieties and the 1-octanol molecules, as shown in Fig. 2. The correlation factors of the regression equations used to calculate the diffusivities of the moieties are also given in Table S1. In this table, the absolute values of the correlation factors exceed 0.99, although the value of the HEMA pentamer (0.978) is smaller. It is difficult to calculate the very slow diffusion rate of the HEMA pentamer with high accuracy, but this figure corroborates that the mobility of the HEMA pentamer is much lower than that of the MEA pentamer. Figure 2 shows that the diffusivities of the MEA/HEMA moieties and 1-octanol molecules decrease with the increasing molecular weights of the moieties. We note that the absolute diffusivities of the HEMA moieties are only 21–46% of the diffusivities of the MEA moieties, even when the molecular weights of the moieties are equal. This consistency suggests lower molecular mobilities of the PHEMA chains compared to those of the PMEA chains in the 1-octanol solvent.

RDF curves for O_M–H_O and O_H–H_O were calculated for the MEA/HEMA oligomers, as shown in Fig. 3a, b. For reference, RDF curves for O_M–O_O and O_H–O_O are also shown in Fig. 3a, b, respectively. Figure 3a exhibits sharp solvation peaks with heights of 1.9–2.5 at ~0.19 nm for O_M–H_O. Peaks with heights of 1.0–1.3 are also observed at ~0.29 nm for O_M–O_O, although these peaks are ascribed to O_M–H_O. Figure 3b exhibits much higher solvation peaks with heights of 6.0–7.8 at ~0.19 nm for O_H–H_O. These peaks are followed by O_H–O_O peaks with heights of 5.4–6.5 at ~0.28 nm. Additional solvation peaks with heights of 1.2–1.7 are observed at ~0.35 nm for O_H–H_O, while there are no peaks at the corresponding distance for O_M–H_O. The two solvation peaks for O_H–H_O corroborate the formation of a hydrogen-bonding network near the terminal hydroxyl groups of the HEMA moieties. Some aggregated structures composed of MEA/HEMA oligomers were observed in the final snapshots of the MD trajectories examined. These aggregations confirm that PMEA and PHEMA inhibit protein adsorption in a similar manner because the weaker affinity between the oligomers and foulant molecules contribute to higher antifouling properties.

The $C_r(t)$ values for O_M–H_O and O_H–H_O were calculated to evaluate the binding strengths between the terminal groups of the monomers and polar groups of the 1-octanol solvent (Fig. 4a, b, respectively). The $C_r(t)$ values at a radius of 0.2 nm exhibited a dramatic decrease to reach zero within 1 ps because the H_O atoms within the sphere were initially centered on the O_M/O_H atom with a radius of 0.2 nm and immediately moved away from the sphere. When the radius was set to 0.7 nm, the decay of the $C_r(t)$ curves slows because a longer time was required for the H_O atoms in the immediate vicinity of the central O_M/O_H atoms at 0 ps to move outside of the sphere. Figure 4a shows that the final $C_r(t)$ value at 0.4 nm is higher than that at 0.3, 0.5, and 0.6 nm. Figure 4b shows that decreases in the $C_r(t)$ values at a radius exceeding 0.2 nm are unexceptionally slow, which corroborates the importance of the affinities of the hydroxyl group of the HEMA moieties for the formation of a hydrogen-bonding network.

The RDFs for C_M–C_O and O_H–C_O were calculated to determine the solvation-density profiles between the terminal groups of the MEA/HEMA moieties and the nonpolar groups of the 1-octanol solvent, as shown in Figure S1; broad peaks with heights of ~1.5 are observed at ~0.4 nm for C_M–C_O, whereas no clear peaks are observed for O_H–C_O. The $C_r(t)$ values for C_M–C_O and O_H–C_O were also calculated to determine binding strengths, as shown in

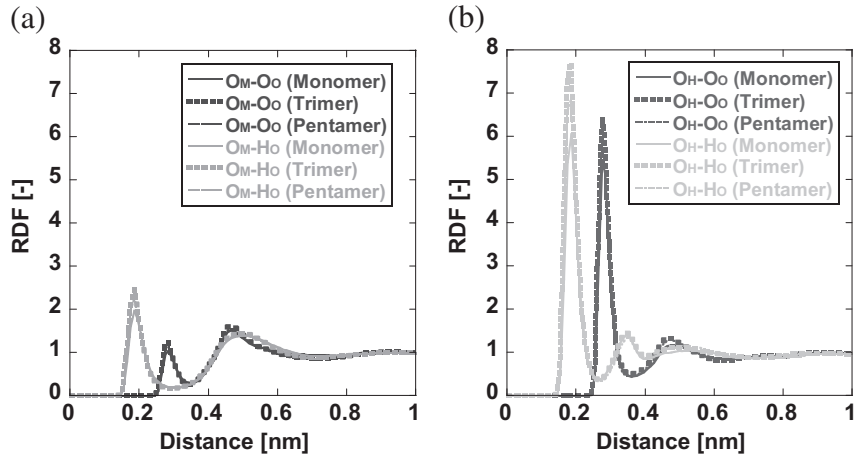

Fig. 3 RDFs of the oxygen atoms (O_O) and hydrogen atoms (H_O) of 1-octanol near (**a**) the oxygen atom (O_M) of the methoxy group in the MEA monomer, trimer, and pentamer and **b** the oxygen atom (O_H) of the hydroxyl group in the HEMA monomer, trimer, and pentamer

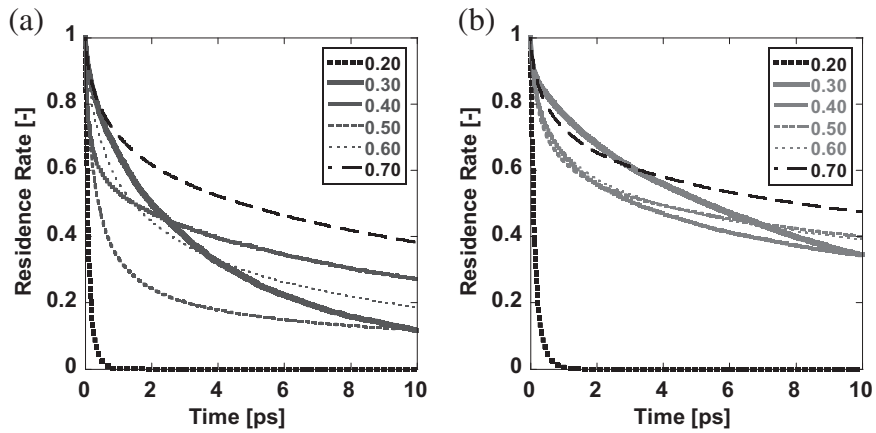

Fig. 4 Residence rates of the oxygen atoms (H_O) of 1-octanol near (**a**) the oxygen atoms (O_M) of the methoxy groups in the MEA moieties and **b** the oxygen atoms (O_H) of the hydroxyl groups in the HEMA moieties. The values shown in the graph legends are the setting radii (nm) for spheres centered at O_M/O_H atoms

Figure S2 (a) and (b), respectively. The $C_r(t)$ curves in Figure S2 (a) are very similar to those shown in Figure S2 (b), although the absolute $C_r(t)$ values in these figures are different. Unless a dynamic property, such as the residence rate, is evaluated, this similarity would remain undetected. Dynamic properties are also essential to accurately determine intermolecular affinities. In addition, this similarity indicates that the intermolecular affinities of the nonpolar groups of the probe foulant do not cause the different molecular mobilities observed in Fig. 2. We suggest that the affinities between the moieties and polar groups of 1-octanol are responsible for this difference.

To evaluate the affinities between the side-chain terminal groups and the polar/nonpolar groups of 1-octanol, the correlations between the residence times and the radii of the spheres centered at C_M/O_H and O_M/O_H were examined, as shown in Fig. 5a, b, respectively. Figure 5a shows the residence times of O_H–C_O and C_M–C_O. No significant differences are observed for the values of the two types of moieties because the $C(t)$ curves shown in Figure S2 (a) and (b) are very similar. This figure confirms that the binding strengths between O_H–C_O and C_M–C_O are almost equivalent. Figure 5b shows the residence times for O_H–H_O and O_M–H_O, where the values for O_M–H_O at radii of 0.35 and 0.45 nm are added. Irrespective of the radius of the sphere, the residence times of O_H–H_O are higher than those of O_M–H_O, confirming that the terminal groups of the HEMA side chains strongly bind the polar hydroxyl groups of 1-octanol. The residence times of O_M–H_O approach those of O_H–H_O, at 0.35–0.40 nm. However, the values of O_M–H_O dramatically decrease above 0.40 nm due to hydrogen bonding between the O_M and H_O atoms, which only provides a local contribution, and the lack of formation of a hydrogen-bonding network near O_M atoms. Steric hindrance by the terminal methyl groups near O_M atoms can interfere with the formation of a network. Attractive interactions between the terminal methyl groups also disturb network formation.

Discussion

Figure 5 shows that the binding strength of O_H–H_O exceeds that of O_M–H_O, suggesting that the affinities of the polar groups of the organic foulant dictate the mobilities of the PMEA and PHEMA chains. The terminal methoxy groups are hydrogen-bond acceptors, but they cannot be the origins

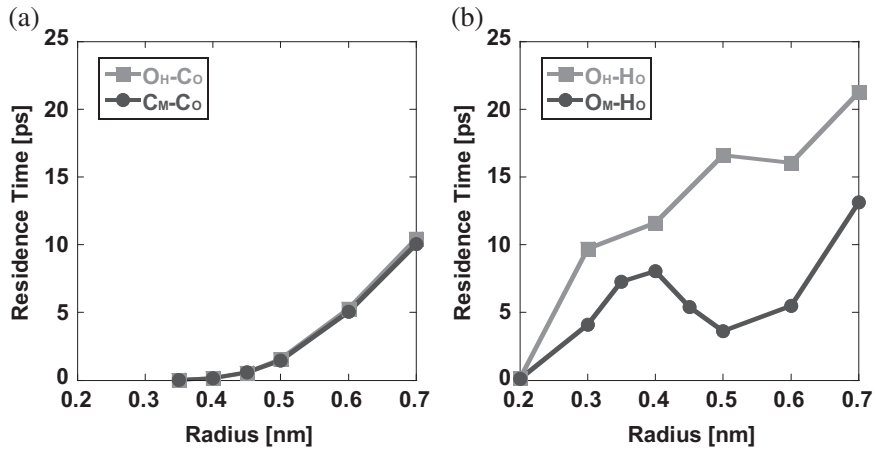

Fig. 5 Relationships between the residence times and setting radii of spheres. **a** The residence times of the carbon atoms (C_O) of 1-octanol near the oxygen atoms (O_H) of the hydroxyl groups in the HEMA moieties and the carbon atoms (C_M) of the methoxy groups in the MEA moieties. **b** The residence times of the hydrogen atom (H_O) of the hydroxyl group in 1-octanol near the oxygen atom (O_H) of the hydroxyl groups in the HEMA moieties and the oxygen atoms (O_M) of the methoxy group in the MEA moieties

of the hydrogen-bonding network between the MEA moieties and the polar groups of the organic compounds, as in the case of the terminal hydroxyl groups of the HEMA moieties. Considering that irrespective of the degree of polymerization, the molecular mobilities of the HEMA moieties are smaller than those of the MEA moieties in Fig. 2, preventing the polar functional groups of the foulants and materials from forming a hydrogen-bonding network is necessary in order to enhance the mobilities of the molecular chains of non-ionic polymeric materials. We speculate that enhancing the mobilities of the molecular chains is key to improving blood compatibility. Calculation of other properties, such as the distribution of the hydrogen-bond number and the hydrogen-bond lifetime, is essential to evaluate the correlation between the mobilities and biocompatibilities at the atomic level. We plan to determine the relationships between the calculated mobilities and the experimental biocompatibilities of various materials, including hydrophilic and hydrophobic oligomers with higher degrees of polymerization.

Acknowledgements This work was supported by the Kurita Water and Environment Foundation (grant no. 15A032) and JSPS KAKENHI (grant no. 16K06825). We thank Editage (www.editage.jp) for English language editing.

Compliance with ethical standards

Conflict of interest The authors declare that they have no conflict of interest.

References

1. Tanaka M, Motomura T, Kawada M, Anzai T, Kasori Y, Shiroya T, et al. Blood compatible aspects of poly(2-methoxyethylacrylate) (PMEA)—relationship between protein adsorption and platelet adhesion on PMEA surface. Biomaterials. 2000;21:1471–81.
2. Tanaka M, Hayashi T, Morita S. The roles of water molecules at the biointerface of medical polymers. Polym J. 2013;45: 701–10.
3. Javakhishvili I, Tanaka M, Ogura K, Jankova K, Hvilsted S. Synthesis of graft copolymers based on poly(2-methoxyethyl acrylate) and investigation of the associated water structure. Macromol Rapid Commun. 2012;33:319–25.
4. Miwa Y, Ishida H, Saitô H, Tanaka M, Mochizuki A. Network structures and dynamics of dry and swollen poly(acrylate)s. Characterization of high- and low-frequency motions as revealed by suppressed or recovered intensities (SRI) analysis of ^{1}3C NMR. Polymer. 2009;50:6091–9.
5. Tanaka M, Sato K, Kitakami E, Kobayashi S, Hoshiba T, Fukushima K. Design of biocompatible and biodegradable polymers based on intermediate water concept. Polym J. 2015;47:114–21.
6. Seo J-H, Yui N. The effect of molecular mobility of supramolecular polymer surfaces on fibroblast adhesion. Biomaterials. 2013;34:55–63.
7. Nagumo R, Ito T, Akamatsu K, Miura R, Suzuki A, Tsuboi H, et al. Molecular dynamics simulations for microscopic behavior of water molecules in the vicinity of zwitterionic self-assembled monolayers. Polym J. 2012;44:1149–53.
8. Nagumo R, Akamatsu K, Miura R, Suzuki A, Hatakeyama N, Takaba H, et al. A theoretical design of surface modifiers for suppression of membrane fouling: potential of poly(2-methoxyethylacrylate). J Chem Eng Jpn. 2012;45:568–70.
9. Nagumo R, Akamatsu K, Miura R, Suzuki A, Hatakeyama N, Takaba H, et al. Computational chemistry study on the microscopic interactions between biomolecules and hydrophilic polymeric materials. J Chem Eng Jpn. 2013;46:421–3.
10. Nagumo R, Terao S, Miyake T, Furukawa H, Iwata S, Mori H, et al. Theoretical screening of antifouling polymer repeat units by molecular dynamics simulations. Polym J. 2014;46:736–9.
11. Nagumo R, Suzuki R, Miyake T, Furukawa H, Iwata S, Mori H. Molecular dynamics study of the correlation between the solvation structures and the antifouling properties of three types of betaine moieties. J Chem Eng Jpn. 2017;50:333–8.
12. Case DA, Betz RM, Cerutti DS, Cheatham III TE, Darden TA, Duke RE, et al. AMBER 2016. San Francisco: University of California; 2016.
13. Wang J, Wolf RM, Caldwell JW, Kollman PA, Case DA. Development and testing of a general AMBER force field. J Comput Chem. 2004;25:1157–74.

14. Jakalian A, Bush BL, Jack DB, Bayly CI. Fast, efficient generation of high-quality atomic charges. AM1-BCC model: I. Method. J Comput Chem. 2000;21:132–46.
15. Jakalian A, Jack DB, Bayly CI. Fast, efficient generation of high-quality atomic charges. AM1-BCC model: II. Parameterization and validation. J Comput Chem. 2002;23:1623–41.
16. Berendsen HJC, Postma JPM, van Gunsteren WF, DiNola A, Haak JR. Molecular dynamics with coupling to an external bath. J Chem Phys. 1984;81:3684–90.
17. Essmann U, Perera L, Berkowitz ML, Darden T, Lee H, Pederson LG. A smooth particle mesh Ewald method. J Chem Phys. 1995;103:8577–93.
18. Al-Jimaz AS, Al-Kandary JA, Abdul-Latif A-HM. Acoustical and excess properties of {chlorobenzene + 1-hexanol, or 1-heptanol, or 1-octanol, or 1-nonanol, or 1-decanol} at (298.15, 303.15, 308.15, and 313.15) K. J Chem Eng Data. 2007;52: 206–14.
19. ChemicalBook Inc. Chemical Book. http://www.chemicalbook.com/ProductList_En.aspx?kwd=methoxyethyl%20acrylate. Accessed 11 Apr 2018.
20. Peschier LJC, Bouwstra JA, de Bleyser J, Junginger HE, Leyte JC. Water mobility and structure in poly[2-hydroxyethylmethacrylate] hydrogels by means of the pulsed field gradient NMR technique. Biomaterials. 1993;14:945–52.